Spontaneous origin from human embryonic stem cells of liver cells displaying conjoint meso-endodermal phenotype with hepatic functions

Sriram Bandi, Kang Cheng, Brigid Joseph and Sanjeev Gupta*

Ruth L. and David S. Gottesman Institute for Stem Cell and Regenerative Medicine Research, Marion Bessin Liver Research Center, Diabetes Center, Cancer Center, Institute for Clinical and Translational Research, and Departments of Medicine and Pathology, Albert Einstein College of Medicine, Bronx, NY 10461, USA

*Author for correspondence (sanjeev.gupta@einstein.yu.edu)

Accepted 14 October 2011
Journal of Cell Science 125, 1274–1283

doi: 10.1242/jcs.095372

Summary

Understanding the identity of lineage-specific cells arising during manipulations of stem cells is necessary for developing their potential applications. For instance, replacement of crucial functions in organ failure by transplantation of suitable stem-cell-derived cells will be applicable to numerous disorders, but requires insights into the origin, function and fate of specific cell populations. We studied mechanisms by which the identity of differentiated cells arising from stem cells could be verified in the context of natural liver-specific stem cells and whether such differentiated cells could be effective for supporting the liver following cell therapy in a mouse model of drug-induced acute liver failure. By comparing the identity of naturally occurring fetal human liver stem cells, we found that cells arising in cultures of human embryonic stem cells (hESCs) recapitulated an early fetal stage of liver cells, which was characterized by conjoint meso-endoderm properties. Despite this fetal stage, hESC-derived cells could provide liver support with appropriate metabolic and ammonia-fixation functions, as well as cytoprotection, such that mice were rescued from acute liver failure. Therefore, spontaneous or induced differentiation of human embryonic stem cells along the hepatic endoderm will require transition through fetal-like stages. This offers opportunities to prospectively identify whether suitable cells have been generated through manipulation of stem cells for cell therapy and other applications.

Key words: Differentiation, Embryonic, Fetal, Liver failure, Stem cells, Therapy

Introduction

The isolation first of human embryonic stem cells (hESCs) (Thomson et al., 1998) and next of induced pluripotential stem cells (iPSCs) (Nakagawa et al., 2008; Wu and Hochedlinger, 2011), generated extensive interest for biological studies, model development, drug and toxicity testing, cell therapy etc. Because hepatocytes have been a major focus of such efforts, understanding mechanisms in the development of foregut hepatic endoderm as well as conversion of lineage-committed cells to mature hepatocytes is of great importance. The nature of genetic regulatory mechanisms driving hepatic specification and differentiation during ontogeny has recently been defined to some extent, especially in model organisms (Zaret, 2008). Organ development during embryonic and fetal stages relies upon cell subsets originating from stem cells; it therefore seems reasonable that ontogenic differentiation cues and signals will be applicable to stem cell differentiation. However, identifying effective ways to differentiate stem cells to generate mature hepatocytes requires much work. In particular, the cell differentiation stages through which stem cells must transition, for example, in generating hepatocytes, has been unclear. Therefore, identification of what might constitute the initial hepatic lineage-specific transition during stem cell differentiation is of the highest significance.

In studies of fetal liver development and of isolated fetal liver stem or progenitor cells, significant differences were noted in these cells compared with mature hepatocytes, including multi-lineage gene expression patterns in fetal cells (Inada et al., 2008a; Inada et al., 2008b). The discovery of an unexpected conjoint meso-endodermal phenotype in fetal liver stem cells, which was characterized by simultaneous expression of epithelial and mesenchymal properties, was in agreement with their ability to generate endodermal and mesodermal lineages, such as adipocytes, osteocytes or endothelial cells, as well as hepatocytes or biliary cells (Inada et al., 2008b). During expansion under cell culture conditions, fetal liver stem cells were found to express mesenchymal genes such as vimentin or α-smooth muscle actin (SMA) better, without loss of expression of the epithelial genes E-cadherin, albumin (Alb), glucose-6-phosphatase (G-6-P), glycogen, cytokeratin (CK)-19, γ-glutamyltranspeptidase (GGT), dipeptidyl peptidase IV (DPPIV), etc. We considered these paradigms to be of potential significance for defining cell differentiation mechanisms in stem-cell-derived cells. One consideration was that cell differentiation steps in natural fetal liver stem cells should have been recapitulated during hepatic differentiation of hESCs. Another consideration was that because the cell differentiation process seems to be regulated by various transcription factors, such as FoxA2, and soluble signals, similar processes should regulate hepatic differentiation in hESCs. Also, identification of hepatic lineage advancement in hESCs should establish whether the

Journal of Cell Science

conjoint meso-endodermal stage encountered in naturally derived fetal liver cells constitutes an obligatory differentiation step.

To evaluate these possibilities, we studied putative mesenchymal stem cells (MSCs) arising spontaneously in cultures of WA-01 hESCs (WiCell Research Institute, Madison, WI), which were shown to be capable of generating adipocytes, bone, cartilage and blood cells (Olivier et al., 2006). Here, we report our findings to indicate similarities in the conjoint meso-endodermal phenotype of hESC-derived cells and cultured fetal human liver stem cells. Despite the relative immaturity of these hESC-derived cells, as indicated by the extent of their hepatic functions in vitro, we found in intact mice with toxic-drug-induced acute liver failure (ALF), that intraperitoneal transplantation of hESC-derived cells rescued various functions in vivo (Bandi et al., 2011). In this situation, hESC-derived cells provided liver support and also aided liver regeneration through secretion of multiple paracrine factors, without the requirement of reseeding the damaged liver with healthy hepatocytes. Therefore, recapitulation in hESC-derived cells of the conjoint meso-endodermal phenotype characteristic of fetal liver stem cells will be important for hepatic differentiation and applications of stem-cell-derived cells.

Results

Characterization of spontaneously originating MSCs in cultures of hESCs showed properties of fetal human liver stem or progenitor cells. We first examined whether putative MSCs that arose spontaneously in cultures of WA-01 hESCs simultaneously express epithelial properties. Remarkably, we observed markers in these cells of mesoderm, as well as endoderm (see below). In view of this conjoint meso-endoderm display, we designated these cells as hESC-derived meso-endoderm cells (hESC-MECs). The morphology of hESC-MECs was different from that of freshly isolated epithelial fetal liver stem cells (FH-Ep-PP), as well as from undifferentiated WA-01 hESCs (Fig. 1). By contrast, the morphology of hESC-MECs resembled that of fetal human epithelial liver stem cells cultured for three (or more) passages (FH-Ep-P3). The hESC-MECs and cultured fetal liver cells showed intermediate filaments, along with cytoplasmic complexity, as well as mitochondria, vacuoles and primary lysosomes, which was consistent with conjoint display of mesenchymal and epithelial properties.

Lineage advancement in hESC-MECs should alter expression of pluripotency-associated genes. Therefore, we immunostained cells for OCT4, SSEA4 and TRA-1-60, and found these genes were expressed at lower levels compared with undifferentiated hESCs (Fig. 2A–C). This finding was similar to that in FH-Ep-P3 cells. Molecular assays with quantitative reverse-transcription polymerase chain reaction (qRT-PCR) showed that hESC-MECs expressed the mesenchymal genes vimentin and α-SMA, as expected, while simultaneously expressing epithelial genes encoding Alb, CK-19 and several Cyp450 genes (Fig. 2D). This was similar to the conjoint meso-endodermal properties in FH-Ep-P3 cells, as previously described (Inada et al., 2008b).

The presence in hESC-MECs of hepatic and biliary markers was confirmed by cytochemical staining for glycogen,

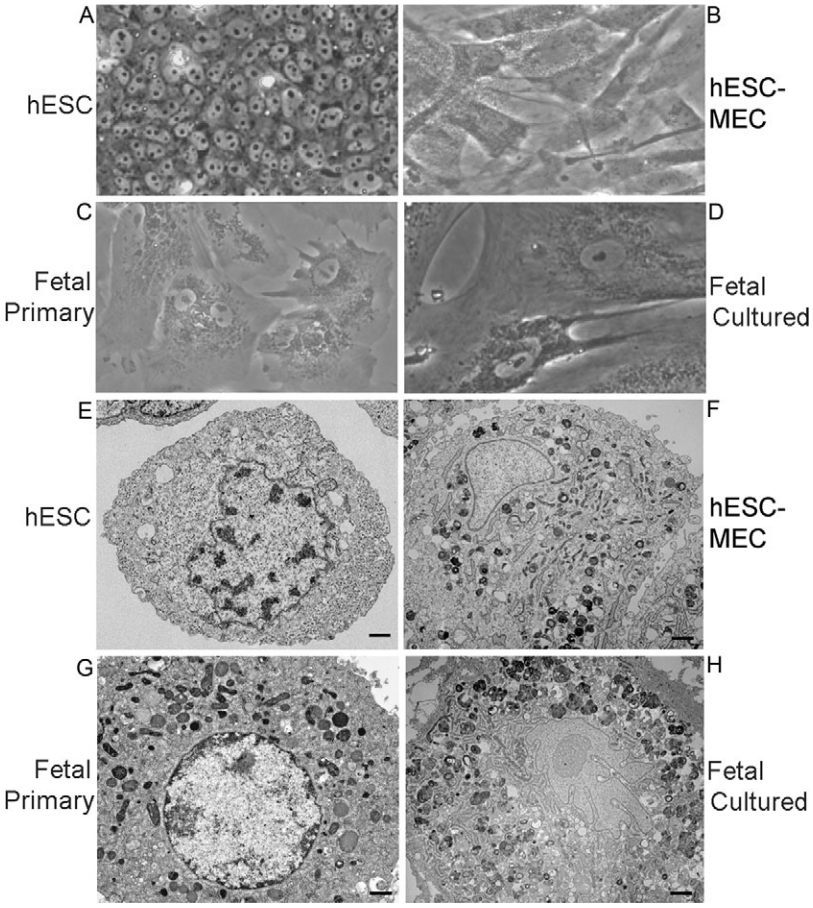

Fig. 1. Morphological properties of cells. (**A**–**D**) Phase-contrast micrographs showing (A) undifferentiated hESCs, (B) hESC-MECs, (C) Ep-CAM-positive primary fetal liver stem cells (FH-Ep-PP) and (D) FH-Ep-P3 fetal liver cells after three passages in culture. (**E**–**H**) Transmission electron microscopy showing undifferentiated hESCs (E), hESC-MECs (F), FH-Ep-PP cells (G) and FH-Ep-P3 cells (H). Morphology of hESCs differs markedly from other cell types, with less cytoplasmic complexity and general lack of cell organelles. hESC-MECs and fetal cells resemble one another, with larger sizes and greater cytoplasmic complexity, including more mitochondria, peroxisomes, lysosomes and vesicles. Magnification: ×600 (A–D). Scale bars: 1 μm.

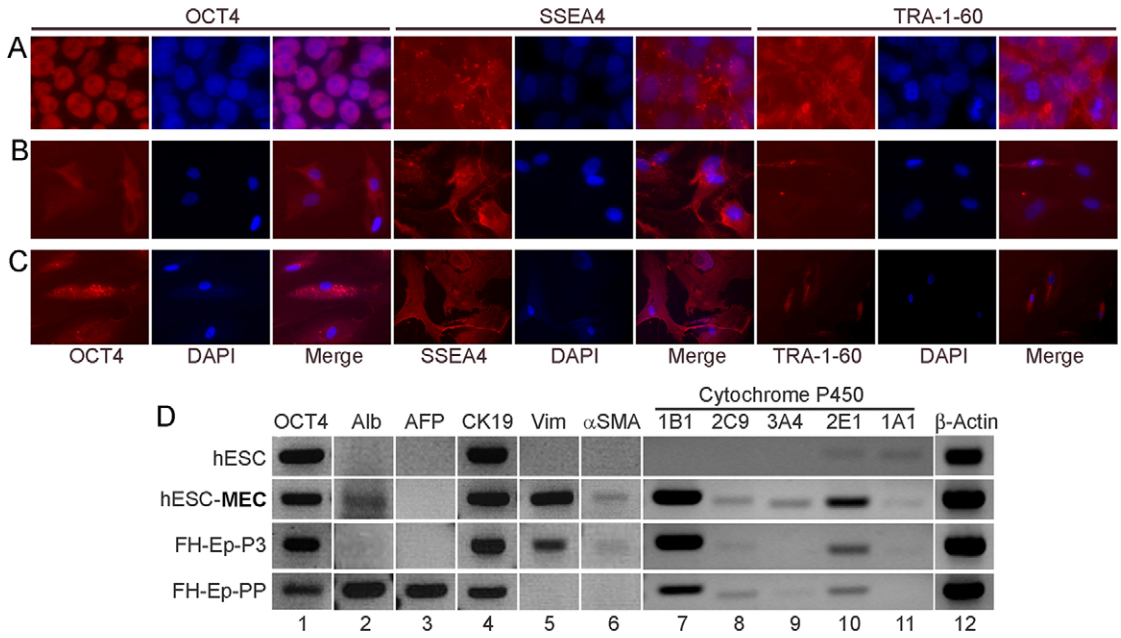

Fig. 2. Characterization of hESC-MECs. (**A**–**C**) Immunostaining for pluripotency markers Oct4, SSEA4 and TRA-1-60 in undifferentiated hESCs (A), hESC-MECs (B) and FH-Ep-P3 cells (C). (**D**) RT-PCR gene expression analysis in hESCs, hESC-MECs, FH-Ep-P3 and FH-Ep-PP cells for the Oct4 marker of pluripotency, hepatobiliary genes Alb, AFP, CK19 and cytochrome P450s as indicated, as well as mesenchymal genes Vim and α-SMA (lanes 1–11). Lane 12 shows expression of the β-actin housekeeping gene.

G-6-P and GGT, whereas the presence of the mesenchymal marker, vimentin, was simultaneously noted (Fig. 3A). Because gene promoters are regulated by cofactors in a cell-type-specific manner, we examined the activity of hepatic promoter constructs after introducing these into hESC-MECs using lentiviral vectors. We found that hESC-MECs were permissive for Alb, transthyretrin (TTR) and α-1-antitrypsin (AAT) promoters; Alb>TTR>AAT (Fig. 3B). This indicated that the intracellular context of hESC-MECs was appropriate for hepatic gene transcription and emphasized that the meso-endodermal state of hESC-MECs in this respect was very similar to that of fetal liver cells (Inada et al., 2008b).

To further determine similarities in various cell populations, we examined genome-wide gene expression by Affymetrix U133 Plus 2.0 Arrays in undifferentiated hESC, hESC-MEC and FH-Ep-P3 cells (supplementary material Fig. S1). The hESC-MECs differed more from undifferentiated hESCs than they did from FH-Ep-P3 cells. When gene expression was compared in hESC-MECs and undifferentiated hESCs, we found that 3780 genes (8%) were upregulated and 4134 genes (9%) were downregulated. This was similar to differences in FH-Ep-P3 cells and undifferentiated hESCs where 4688 genes (10%) were upregulated and 4951 genes (10%) were downregulated. By contrast, in the comparison of hESC-MECs and FH-Ep-P3 cells, fewer genes were either upregulated [2115 genes (4%)] or downregulated [2332 genes (5%)] ($P<0.05$). Therefore, although global gene expression patterns in hESC-MECs and FH-Ep-P3 cells were not identical, these cell types were more divergent from undifferentiated hESCs than from one another. This convergence of gene expression was substantiated by similarities in hESC-MECs and FH-Ep-P3 of cytokine-signaling networks directing cell differentiation, e.g. transforming growth factor (TGF)-β or bone morphogenetic protein (BMP) pathways, which control mesenchymal differentiation (supplementary material Fig. S1). Also, we compared gene expression levels from an Affymetrix microarray data of 43 individual genes, including pluripotency genes, and genes indicating advancement along mesoderm, endoderm, and hepatic lineages (supplementary material Table S1). This confirmed that pluripotency genes were downregulated in hESC-MECs compared with undifferentiated hESCs. By contrast, expression of mesoderm, endoderm, and hepatic genes in hESC-MECs was similar to levels in FH-Ep-P3 cells (supplementary material Table S2).

An array-based analysis of more than 500 cellular microRNAs (miRNAs), including those involved in stem cell differentiation, showed broad convergences of expression in hESC-MECs and FH-Ep-P3, and divergences from undifferentiated hESCs (supplementary material Fig. S2). Moreover, miRNA expression profiles in hESC-MECs were closer to those of primary fetal liver cells, although not identical (supplementary material Fig. S3). This emphasized the immaturity of both hESC-MECs and FH-Ep-P3 cells. Nonetheless, considered together, these findings establish that hESC-MECs belong in an early meso-endoderm stage of natural fetal liver cells.

The differentiation potential of hESC-MECs recapitulated that of fetal human liver stem cells. To study the differentiation capacity of hESC-MECs, we induced osteogenic, adipogenic and endothelial lineages by established protocols over 3 weeks in vitro (supplementary material Fig. S4) (Dan et al., 2006; Inada et al., 2008b; Ria et al., 2008). The hESC-MECs generated osteocytes, adipocytes and endothelial-like cells, which is similar to the differentiation ability of fetal human liver stem cells (Inada et al., 2008b).

Next, we determined whether hepatic differentiation in hESC-MECs was advanced by cytokine inducers of endoderm, e.g. activin A, acidic fibroblast growth factor (FGF), hepatocyte

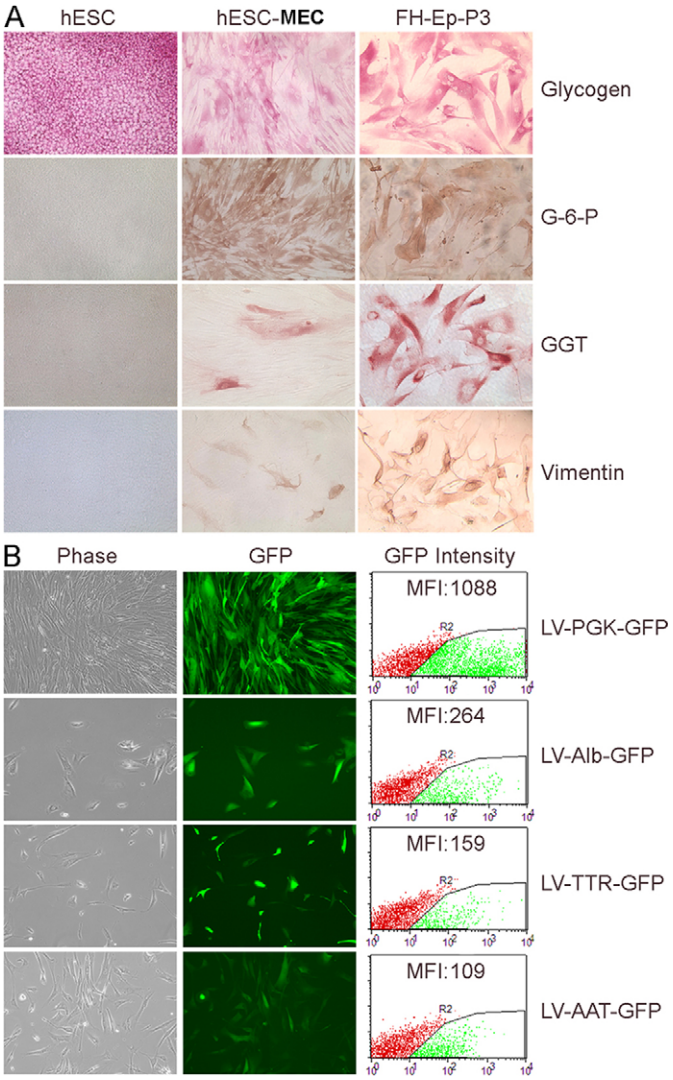

Fig. 3. Mesenchymal and hepatic properties in hESC-MECs. (**A**) Cytostaining in hESCs, hESC-MECs and FH-Ep-P3 cells for hepatobiliary markers glycogen, G-6-P and GGT, and the mesenchymal marker vimentin. hESCs stained for glycogen. hESC-MECs and FH-Ep-P3 cells display similar properties. (**B**) hESC-MECs transduced with lentiviral vectors (LV) with Alb, TTR and AAT promoters driving GFP expression. Left, phase-contrast microscopy; middle, GFP expression; right, flow cytometry of mean fluorescence intensity (MFI) showing PGK>Alb>TTR>AAT.

growth factor (HGF), oncostatin M, the Wnt antagonist DKK-1, the Notch antagonist γ-secretase inhibitor X or the histone deacetylase inhibitor trichostatin A. After culturing hESC-MECs for 3 weeks with these substances, we examined changes in the hepatobiliary markers glycogen, DPPIV, GGT, Alb, α-fetoprotein and hepatic nuclear factors. However, various combinations of these cytokines failed to increase hepatic differentiation in hESC-MECs (supplementary material Table S3). This too was similar to the lack of their efficacy in FH-Ep-P3 cells. Although protocols incorporating activin A have been particularly successful for endoderm differentiation in hESCs (Phillips et al., 2007), this inefficacy of activin-A-based protocols in hESC-MECs and FH-Ep-P3 cells indicated fundamental differences of these cells from hESCs.

The capacity of hESC-MECs to support liver function in the setting of ALF was elucidated in a drug toxicity model. We considered that the presence of crucial liver proteins glycogen, G-6-P and Cyp450 in hESC-MECs should permit these cells to rescue animals in ALF. We addressed this possibility in xenotolerant natural-onset diabetes-severe combined immunodeficiency (NOD/SCID) mice with ALF induced by a regimen of the hepatotoxic drugs rifampicin (Rif) and phenytoin (Phen), over 3 days, followed on day 4 by the pyrrolizidine alkaloid, monocrotaline (MCT) (Bandi et al., 2011). This produced 50–70% liver necrosis, abnormal liver tests, coagulopathy, encephalopathy and 90–100% mortality, over several days (Fig. 4A). Previously, mice with ALF were rescued after transplantation in the peritoneal cavity of xenogeneic mature hepatocytes anchored to extracellular-matrix-coated microcarriers. In this system, transplanted hepatocytes adhering to microcarriers are revascularized in the peritoneal cavity, along with secretion of proteins in blood (Demetriou et al., 1986; Gupta et al., 1994; Bandi et al., 2011). Moreover, cells transplanted into the peritoneal cavity do not migrate to other organs, including the liver (Bandi et al., 2011). Furthermore, in this ALF model, reseeding of the damaged liver with healthy hepatocytes was not required for liver regeneration (Bandi et al. 2011). After inducing ALF, we subjected mice to transplantation of 4–6 $\times 10^6$ hESC-MECs ($n=11$); 5×10^6 HeLa human cervical cells (irrelevant control) ($n=10$); or vehicle alone (sham treatment) ($n=9$). Over 2 weeks, all 11 mice treated with hESC-MECs survived (100%), whereas only two sham-treated mice survived (22%), and none of the HeLa-treated mice survived (0%) ($P<0.001$, ANOVA; Fig. 4B). We measured blood glucose in several mice and excluded hypoglycemia as a cause of death. None of the mice treated with hESC-MECs showed encephalopathy, whereas sham-treated or HeLa-treated mice developed advanced (grade III–IV) encephalopathy ($P<0.05$). We identified transplanted hESC-MECs by PCR for human sex-determining Region Y (SRY; Fig. 4C) (Wang et al., 2002). In 2 of 11 mice with ALF, 2 weeks after transplantation of hESC-MECs, we detected 0.21–0.48 ng/ml human albumin in blood (normal, 40 μg/ml), whereas human albumin was absent in sham-treated or HeLa-treated mice. This production of albumin in small amounts by transplanted hESC-MECs was in agreement with the hepatic immaturity of these cells.

In sham-treated mice, the liver was grossly abnormal, with edema and hemorrhagic necrosis, whereas the liver in mice treated with hESC-MECs appeared healthy (Fig. 5A). In comparison with sham-treated mice (Fig. 5B), after transplantation of hESC-MECs, liver histology substantially reverted to normal and the prevalence of Ki67-expressing hepatocytes increased, indicating greater liver regeneration (Fig. 5C). Moreover, although sham-treated mice exhibited evidence for significant oxidative DNA damage, as indicated by immunostaining of the liver for phosphorylated histone H2AX, a well-established marker of double-stranded DNA breaks, this parameter decreased in hESC-MEC-treated mice. Therefore, we analyzed whether genes included in pathways of hepatic stress and toxicity were expressed differently in animals 3 and 7 days after ALF. For this, qRT-PCR was performed with arrays of 84 genes in sham-treated and hESC-MEC-treated mice ($n=3$ each). Significant oxidative stress and hepatotoxicity was observed in sham-treated mice, along with perturbations in Cyp450 and other metabolic genes, chemokines and cell cycle

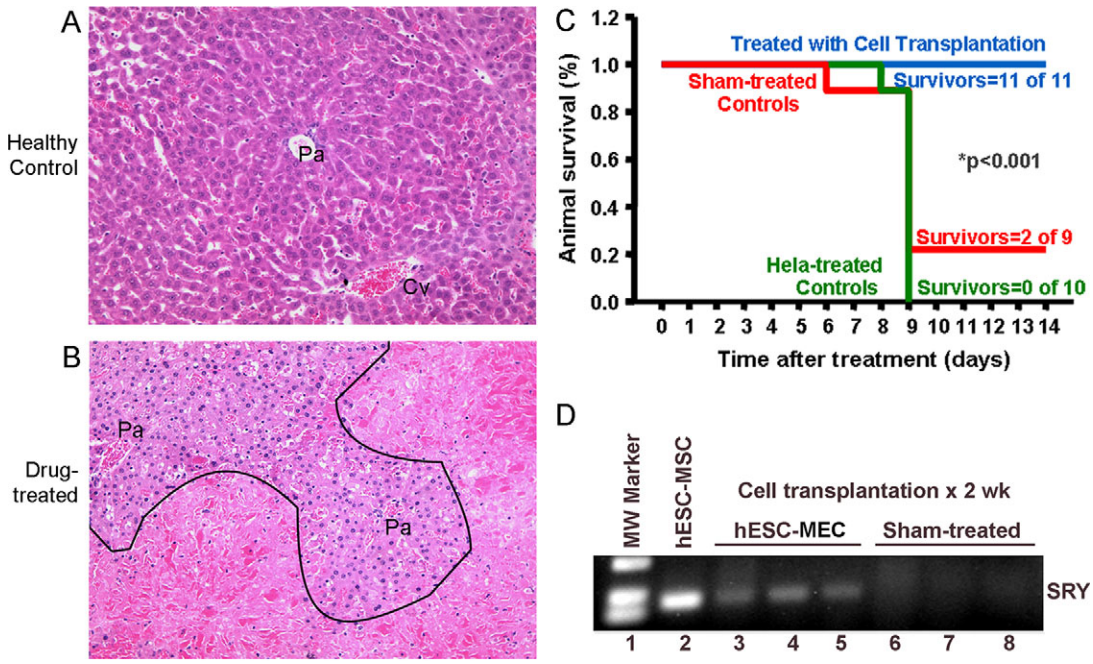

Fig. 4. Changes in hepatic histology during ALF and outcomes after cell transplantation. (**A**) Normal architecture of the liver acinus in control NOD/SCID mouse with portal area (Pa) and central vein (Cv) interspersed with healthy hepatocytes. (**B**) Liver from NOD/SCID mouse 3 days after Rif, Phen and MCT treatment. Extensive hepatic necrosis is seen in perivenous areas (below black line) and intact hepatocytes adjacent to portal areas (above black line). After cell transplantation, the liver regenerates through proliferation of residual hepatocytes. Hematoxylin and eosin stain. Magnification: ×200. (**C**) Survival curves in NOD/SCID mice with ALF. All animals treated with hESC-MECs survive, whereas recipients of HeLa cells and sham-treated mice show mortality of 78–100%. (**D**) Identification of human cells in mice with genomic DNA PCR for SRY. Lane 1, molecular size marker; lane 2, cultured hESC-MECs as positive control; lanes 3–5, mice transplanted with hESC-MECs; and lanes 6–8, sham-treated mice without SRY band.

checkpoint controls (e.g. p21), whereas these changes were either attenuated or resolved altogether in mice treated with hESC-MECs (supplementary material Table S4). This was in agreement with excellent hepatic recovery after cell therapy with hESC-MECs.

We identified transplanted human cells in the peritoneal cavity of treated mice by in situ hybridization with a pancentromeric human probe (Benten et al., 2006) (Fig. 6A–D). Transplanted cells had not migrated to the liver. Transplanted hESC-MECs contained glycogen and G-6-P, whereas these hepatic markers were absent in HeLa cells, as expected. We did not observe mesodermal lineages such as cartilage or bone formation in vivo. Similarly, we did not observe any endothelial or tubular structures derived from transplanted cells that had been identified by in situ hybridization for pancentromeric sequences.

Transplantation of hESC-MECs transduced with Alb–GFP lentiviral vector confirmed hepatic function in hESC-MECs in vivo (Fig. 7A–F). Similarly, transplantation of hESC-MECs into the liver of NOD/SCID mice demonstrated that cells engrafted in the liver parenchyma and contained glycogen, which was again in agreement with their capacity to express hepatic functions in vivo. Intraperitoneal or intrahepatic transplantation of hESC-MECs in NOD/SCID mice did not produce neoplasia after 2 weeks ($n=10$). Transplanted cells did not form large clusters to indicate progressive proliferation and remained relatively limited in numbers around microcarriers. In formal assays of tumorigenicity, we injected hESC-MECs subcutaneously in NOD/SCID mice ($n=10$), and did not observe any tumors over at least 3 months. This was in agreement with their divergence from undifferentiated hESCs, which produced teratomas in all cases within one week after intraperitoneal, intrahepatic or intrasplenic transplantation ($n=3$ each; Fig. 7G–I).

To determine whether hESC-MECs could rescue mice with even more severe ALF, we repeated cell transplantation studies in mice treated with Rif, Phen and more MCT (160 mg/kg). In this situation, 38% of mice treated with hESC-MECs survived versus 13% of sham-treated mice over 2 weeks ($n=8$ each; $P<0.05$; Fig. 8A). To define whether mice with ALF were rescued by hepatic support from transplanted hESC-MECs or through paracrine effects from proteins secreted by transplanted cells, we treated mice receiving Rif, Phen and 160 mg/kg MCT ($n=10$), followed by three doses of conditioned medium from hESC-MECs ($n=4$) or basal medium ($n=6$). Characterization of this conditioned medium with a cytokine array demonstrated the presence of multiple cytokines (supplementary material Fig. S5). However, conditioned medium alone did not improve survival of mice (Fig. 8B), indicating that intact hESC-MECs are necessary for liver support. This study was limited by intermittent dosing of conditioned medium over 3 days, whereas transplanted cells would have continuously released paracrine factors over the entire duration of the study. Next, to elucidate the extent of hepatic functions in hESC-MECs, we studied Cyp450 activity, ureagenesis and albumin secretion in comparison with levels in HepG2 (human hepatoblastoma) cells, which have been of interest for bioassist liver devices (Massie et al., 2011). The capacity of hESC-MECs to convert ethoxyresorufin was greater than HepG2 cells under baseline conditions, although hESC-MECs did not show further induction by phenobarbital of

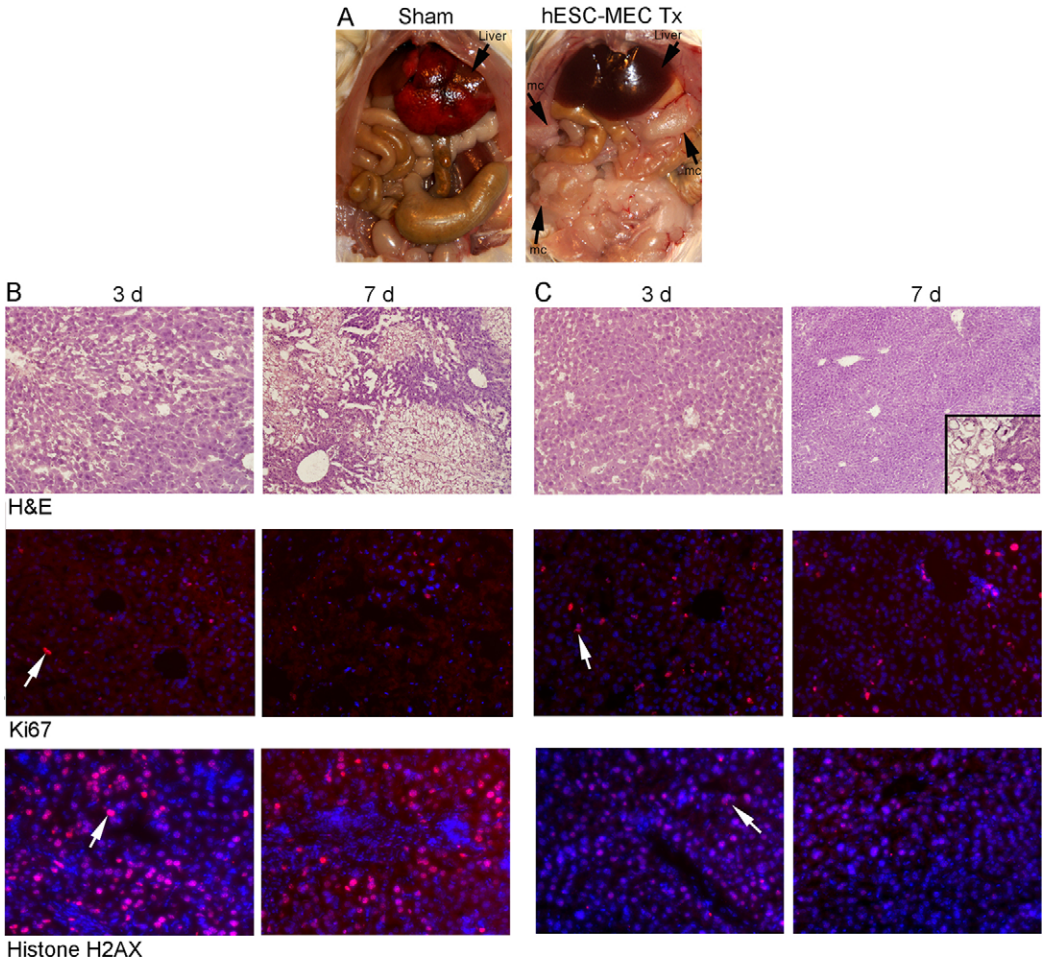

Fig. 5. Liver regeneration after transplantation of hESC-MECs. (**A**) Gross appearance of abdominal organs in sham-treated and hESC-MEC-treated mice. Note extensive liver edema and necrosis in sham-treated mouse after 2 weeks compared with normal appearing liver in hESC-treated mice. Arrows indicate conglomerates of transplanted cells and microcarriers (mc). (**B**,**C**) Liver histology with extensive necrosis and oxidative DNA damage in sham-treated mice after 3 days and 7 days (B), along with less necrosis, liver regeneration and decreased DNA damage in mice after cell transplantation (C). Top, H&E staining. Inset in C shows magnified view of transplanted cells with microcarriers. Middle, Ki67 staining (red) of liver with DAPI counterstaining of nuclei (blue) to indicate extent of regenerative activity. Bottom, staining for phosphorylated histone H2AX (red) as a marker of oxidative DNA damage with DAPI counterstaining of nuclei (blue). Arrows indicate examples of Ki67- or H2AX-positive cells. Magnification: ×100 (B), ×200 (C).

Cyp450 activity, which was different from this response of HepG2 cells (Fig. 8C). hESC-MECs synthesized urea at a similar level to that in HepG2 cells (Fig. 8D). However, hESC-MEC did not secrete Alb in detectable amounts in the culture medium, even though in animals with ALF, human albumin was detected following transplantation of hESC-MECs. To determine whether paracrine factors secreted by hESC-MECs could have protected the native liver, we studied conditioned medium from hESC-MECs, and found that this protected primary mouse hepatocytes from TNF-α-induced cytotoxicity (Fig. 8E). Studies with vascular endothelial growth factor (VEGF), which was present in conditioned medium from hESC-MECs, showed that VEGF protected hepatocytes from TNF-α-induced cytotoxicity (Fig. 8F), which further substantiated the role of paracrine factors.

Discussion

These findings establish that putative MSCs arising spontaneously during culture of hESCs actually represent the equivalent of naturally occurring fetal liver cells, which display conjoint meso-endoderm properties. This was established in multiple ways, including similarities at the levels of morphology, ultrastructure, phenotypic markers, gene expression profiles, as well as presence of hepatic functions in cells, despite the simultaneous expression of mesenchymal markers. Moreover, hESC-MECs showed a capacity to rescue animals with liver failure by providing hepatic functions and by promoting liver regeneration through paracrine factors. This identification of hepatic endoderm generation in hESCs should be important for further analysis of cell differentiation mechanisms, as well as for applications of hESC-derived cells.

Our prediction was that if hESC-MECs represent endodermal cells, these will share their identity with naturally occurring fetal human liver stem cells (Inada et al., 2008a). This was confirmed by multiple assays as described above. The meso-endoderm state of hESC-MECs and of fetal human liver stem cells resembled the meso-endodermal phenotype of cells during embryonic gastrulation, although those cells have not been as well

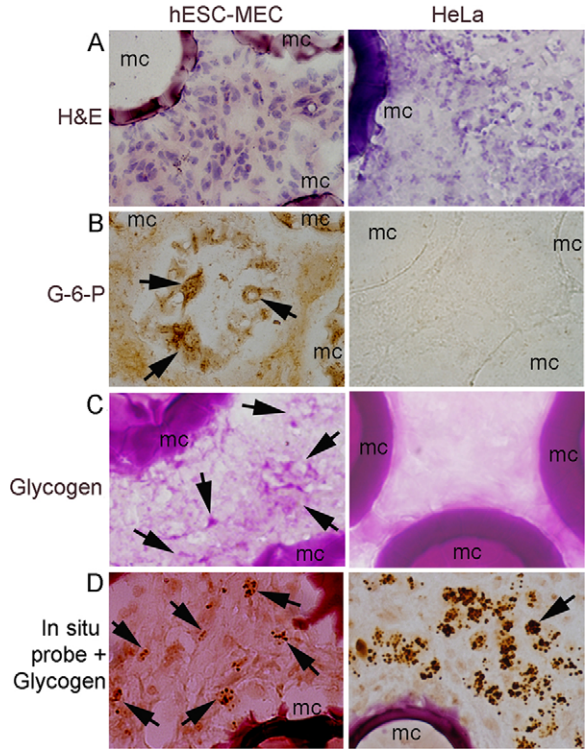

Fig. 6. Identification of transplanted cells. (**A**) hESC-MECs and HeLa cells with mouse stroma adjacent to microcarriers (mc); hematoxylin staining. (**B**) G-6-P shown by enzyme histochemistry in transplanted hESC-MECs (arrows, brown cytoplasm). G-6-P is not expressed in HeLa cells. (**C**) Glycogen is present in hESC-MECs (arrows, pink cytoplasm), but is absent in HeLa cells, as expected. (**D**) In situ hybridization with pancentromeric human probe combined with glycogen staining to verify presence of transplanted cells. These are covered with dark hybridization signals (arrows). Magnification: ×600.

characterized. Also, our studies provided experimental support for the likely origin of mesoderm and endoderm from shared meso-endoderm precursor cells, as had previously been contemplated (Rodaway and Patient, 2001). The expression at lower levels of pluripotency-associated genes OCT4, SSEA4 and TRA-1-60 in hESC-MECs, as well as in fetal liver stem cells, was in agreement with their departure from the stem cell stage as a result of the onset of lineage specification and progression. The findings suggest that induction of differentiation in hESCs (or iPSCs) along this meso-endoderm state should provide opportunities for insights in endoderm specification, commitment and advancement. Identification of early steps in hepatic endoderm development should be particularly helpful for derivation of hepatic lineages and thus will benefit translational applications of stem cells, including for disease models and toxicological systems.

Despite their immature state, hESC-MECs perform crucial hepatic functions, such as glycogen storage, glucose metabolism, xenobiotic disposal through Cyp450 activity, and ammonia fixation through ureagenesis, which are considered essential for hepatic support in ALF, as was substantiated by rescue of mice with ALF. However, transplanted hESC-MECs provided paracrine signals capable of interfering with hepatotoxicity, as indicated by studies of TNF-α-induced cytotoxicity. Of course, correction of genetic diseases or other conditions by proteins normally produced in adult hepatocytes (Fisher and Strom, 2006), will require further hepatic maturation in hESC-MECs or equivalent cells. Our efforts to advance hepatic maturation in hESC-MECs with soluble signals were unsuccessful, indicating that this area needs more work. Although we observed the ability of hESC-MECs to generate additional lineages under suitable differentiation conditions in vitro (e.g. endothelial cells), we did not observe hESC-MEC-derived non-hepatic cell types in vivo. Whether such hESC-MEC-derived non-hepatic lineages could be useful for supporting liver regeneration through additional

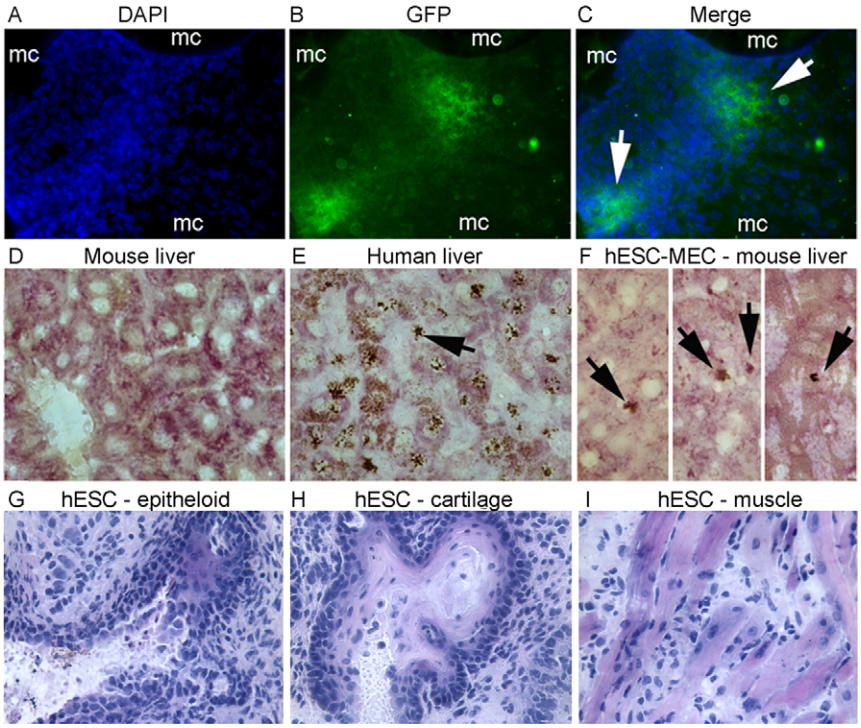

Fig. 7. Hepatic functions in transplanted hESC-MECs. (**A**–**C**) hESC-MECs transduced with lentiviral vectors containing the Alb promoter to drive GFP expression. Cells were transplanted with microcarriers (mc) into peritoneal cavity in NOD/SCID mice. Two weeks later, conglomerates of transplanted cells and mc were recovered for GFP immunostaining. DAPI staining visualized nuclei (A, blue), GFP staining verified albumin promoter activity (B, green) and merged image (C) shows both properties with transplanted hESC-MECs adjacent to microcarriers (arrows). (**D**–**F**) Colocalization of glycogen in hESC-MECs transplanted via the portal vein into liver of NOD/SCID mice followed 5 days later by analysis of liver sections for glycogen plus in situ hybridization with human pancentromere probe and color development with diaminobenzidine. (D) Cytoplasmic glycogen in mouse liver without cell transplantation and absence of in situ signals for human sequences. (E) Glycogen and nuclear hybridization signals in human liver (arrow). (F) hESC-MECs in mouse liver with glycogen and in situ hybridization signals for human sequences (arrows). (**G**–**I**) Transplantation of undifferentiated hESCs in the spleen, liver or peritoneal cavity produces teratomas with derivatives of multiple germlayers, including epithelial and mesenchymal cells, as shown. Magnification: ×400.

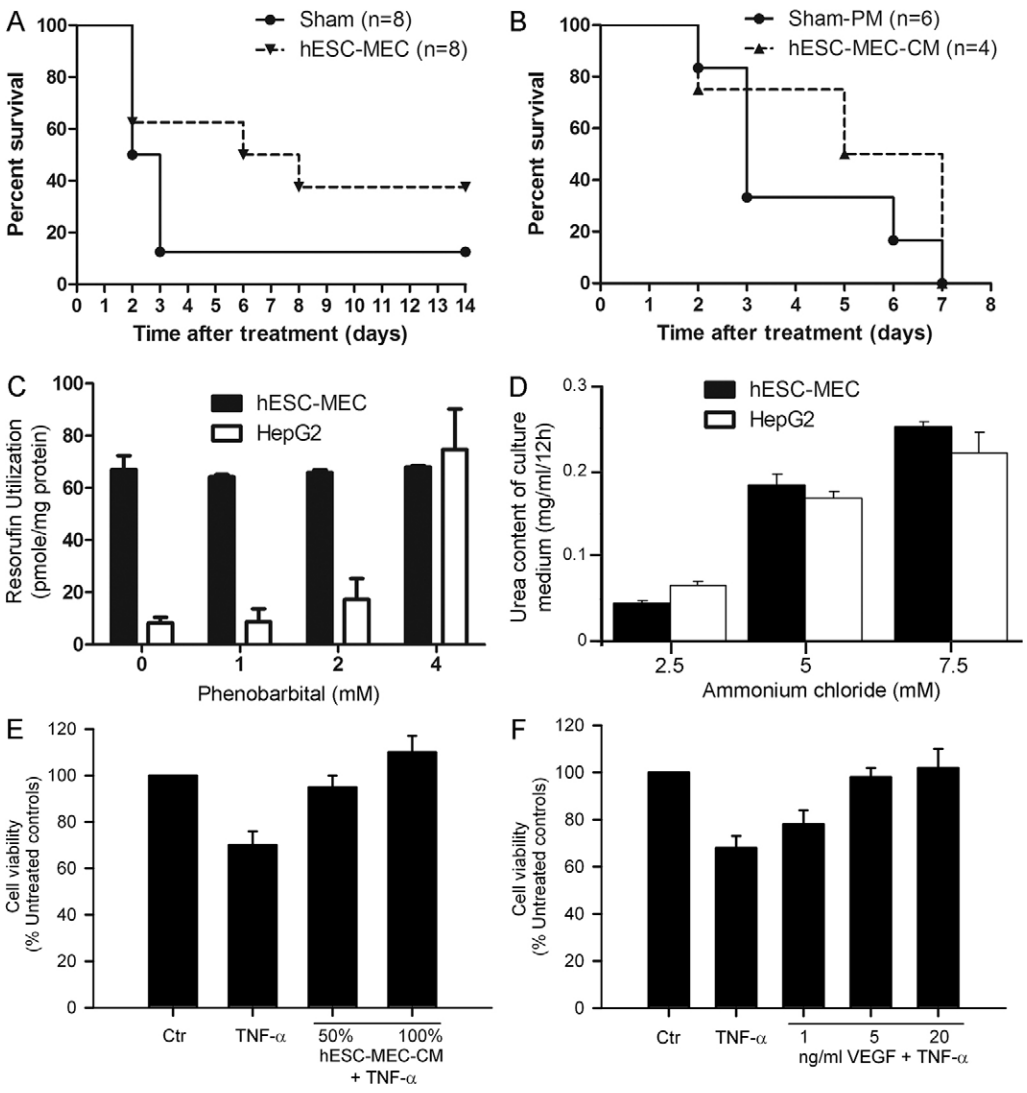

Fig. 8. Outcomes in mice with severe ALF and effects of conditioned medium. (**A**) Survival in mice given Rif, Phen and 160 mg/kg MCT followed by either sham treatment or transplantation of hESC-MECs ($n=8$ each). Seven of eight sham-treated mice died 3 days after MCT treatment. By contrast, mortality is lowered in mice treated with 5×10^6 hESC-MECs. (**B**) Survival in ALF after administration of plain medium (PM) or conditioned medium from hESC-MECs. Mice were treated by intraperitoneal injection of 1 ml medium daily commencing 1 day after Rif, Phen and 125 mg/kg MCT and continuing until death. Conditioned medium from hESC-MECs did not alter mortality. (**C**,**D**) Hepatic metabolic and synthetic functions in hESC-MECs compared with HepG2 cells with conversion of ethoxyresorufin (C) and urea synthesis (D). (**E**) Cytoprotection with conditioned medium from hESC-MECs of primary mouse hepatocytes cultured with TNF-α. (**F**) The protective effect of VEGF upon TNF-α-induced cytotoxicity is demonstrated to establish that specific constituents released by hESC-MECs are responsible for rescue in ALF. Values plotted in C–F are means ± s.d.

paracrine signaling, as observed after transplantation of endothelial cells (Ding et al., 2010), will require further study.

The establishment of mechanisms explaining how hESC-derived early stage fetal-liver-like cells rescued animals with toxic-drug-induced ALF should be particularly helpful, because drug toxicity is the leading cause of ALF in the western world. Our approach using microcarriers to support transplanted cells in the peritoneal cavity was successful in rescuing animals with ALF. We found that this permitted hESC-derived cells to engraft, survive and function in animals, which provided time for regeneration of the native liver. Previously, mechanisms of liver regeneration following hepatocyte transplantation in ALF were uncertain (Baumgartner et al., 1983; Grundmann et al., 1986; Makowka et al., 1980). Here, we found that transplantation of intact hESC-MECs was necessary for rescuing animals with ALF. Although hESC-MECs secreted several cytokines, conditioned medium containing those cytokines alone did not rescue animals with ALF. This difference from previous studies might be due to more human-like liver injury in our NOD/SCID mouse model of ALF. The role of ataxia telangiectasia mutated (ATM) signaling pathways in oxidative stress, DNA damage and p21-dependent checkpoint controls has been defined in this model (Bandi et al., 2011). The ability of residual hepatocytes in this model to regenerate the liver reproduces the clinical situation in humans, where significant liver regenerative activity is observed, despite terminal ALF (Quaglia et al., 2008).

Therefore, the therapeutic potential of hESC-derived cells recapitulating an early stage in fetal liver development should be attractive for clinical applications of stem cells. For instance, cell transplantation in the peritoneal cavity is far simpler than reseeding the liver with cells, which requires hazardous and invasive means for cell transplantation. Also, the need for only short-term liver support in ALF should permit applications of pre-prepared and frozen cells derived from allogeneic stem cells, aided by further insights in mechanisms of hepatic maturation.

Materials and Methods

The Committee on Clinical Investigations (Institutional Review Board), Embryonic Stem Cell Research Oversight Committee, as well as Animal Care and Use Committee of Albert Einstein College of Medicine approved studies in accordance with institutional, state and federal guidelines.

Fetal tissues

Fetal human livers at 19–24 weeks of gestation were from the Human Fetal Tissue Repository, Albert Einstein College of Medicine. Ep-CAM-positive fetal liver

stem cells were isolated by immunomagnetic beads and cultured as described previously (Inada et al., 2008b).

Cells and cell culture

hESCs were cultured on irradiated feeder cells in DMEM/F12 medium, 20% knock-out Serum Replacer (KSR), 2 mM L-glutamine, 0.1 mM MEM Non Essential Amino Acids Solution (NEAA), 1% penicillin-streptomycin (Invitrogen, Carlsbad, CA), and 4 ng/ml basic FGF (R&D Systems, Minneapolis, MN) (complete medium). Cells were passaged each week. hESC-MECs were obtained by spontaneous differentiation in DMEM with 10% FBS as described previously (Olivier et al., 2006). For conditioned medium, hESC-MECs were cultured for 24 hours in complete medium followed by in DMEM for 24 hours, which was harvested and passed through a 0.22 μm filter (Millipore, Billerica, MA).

Differentiation of hESC-MECs

To induce osteogenic and adipogenic differentiation, cells were cultured in DMEM with 10% FBS and additives for 3 weeks (Inada et al., 2008b; Olivier et al., 2006). For endothelial differentiation (Ria et al., 2008), cells were cultured on fibronectin (Sigma, St Louis, MO). For endoderm differentiation, cells were cultured in RPMI 1640 medium without serum for 2 days, 0.2% serum for 2 days and 2% serum for 2 weeks, with activin A (100 ng/ml), a-FGF (100 ng/ml), HGF (20 ng/ml), OSM (20 ng/ml), DKK-1 (20 ng/ml) (R&D Systems), trichostatin A (100 nM/ml), and γ-secretase inhibitor X (Calbiochem, La Jolla, CA) (supplementary material Table S3).

Immunohistochemistry

Cells were fixed in 4% paraformaldehyde in PBS (PAF) and blocked and permeabilized with 0.2% Triton X-100 and 5% goat serum (Sigma) in PBS for 1 hour, and incubated overnight at 4℃ with mouse antibodies against human Oct3/4 (1:200, Santa Cruz Biotechnology, Santa Cruz, CA), SSEA4 (1:50, R&D Systems), TRA-1-60 (1:50; Chemicon International, Temecula, CA). After washing with PBS, cells were incubated for 1 hour with TRITC-conjugated goat anti-mouse IgG (1:50, Sigma) and counterstained with 4′-6-diamidino-2-phenylindole (DAPI) (Invitrogen). In negative controls, primary antibodies were omitted. Glycogen, G-6-P, GGT and DPPIV were stained as previously described (Inada et al., 2008b).

Electron microscopy

Cells were fixed in 2.5% glutaraldehyde in cacodylate butter, post-fixed in osmium tetroxide, and stained with 1% uranyl acetate before embedding in plastic. Ultrathin sections were examined under JEOL 1200 electron microscope.

Molecular studies

RNA was extracted by TRIzol reagent (Invitrogen), cleaned by RNeasy (Qiagen Sciences, Germantown, MD), incubated in DNase I (Invitrogen) and reverse-transcribed by Omniscript RT kit (Qiagen). Platinum PCR SuperMix (Invitrogen) was used for PCR with annealing at 94℃ for 5 minutes, and 35 cycles of 94℃ for 30 seconds, 55℃ for 30 seconds, 72℃ for 45 seconds and 72℃ for 10 minutes. Primers are listed in supplementary material Table S5.

Mouse Stress and Toxicity RT^2 Profiler PCR Array and RT^2 Real-Time SyBR Green PCR mix and RT^2 First Strand kit were from SABiosciences (Frederick, MD). cDNA synthesis and PCR was according to the manufacturer. Data were analyzed by the 2-ΔΔCt method. Fold-changes in gene expression were expressed as log-normalized ratios from sham-treated to normal and cell transplantation to normal livers. Gene expression was analyzed with U133 2.0 Plus oligonucleotide arrays (Affymetrix, Santa Clara, CA) as described (Inada et al., 2008b). Differentially expressed genes were analyzed by SAS software (SAS Institute, Cary, NC). Gene lists were annotated with DAVID (National Institute of Allergy and Infectious Disease, Bethesda, MD) and gene pathways were according to Kyoto Encyclopedia of Genes and Genomes (KEGG). Specific pathways in differentially expressed gene lists were obtained by PathwayStudio 5.0 (Aridane Genomics, Rockville, MD). For microRNA analysis, total RNA was isolated by TRIzol reagent (Invitrogen), followed by microfluidics arrays (LC Sciences, Houston, TX) with probes from the Sanger database, version 9.0.

Gene transfer

Lentiviral vectors expressing green fluorescent protein (GFP) under PGK, mouse albumin enhancer-promoter, transthyretrin (TTR) and α-1-antitrypsin promoters were prepared (Inada et al., 2008a). Cells were transduced with lentiviral vectors at multiplicity of infection (MOI) of 10. GFP expression was analyzed after 4 days by fluorescence microscopy and flow cytometry.

Biochemical assays

For ureagenesis, cells were incubated with 2.5–7.5 mM ammonium chloride for 12 hours. To 0.6 ml of culture medium was added 0.3 ml of urease (Sigma) for 20 minutes at room temperature followed by 0.6 ml of phenol nitroprusside and alkaline hypochlorite (Sigma), and 3 ml water, and incubation for 30 minutes at room temperature to develop color. Absorbance was measured at 540 nm against a standard curve (Cho et al., 2004). To induce Cyp450 activity, cells were cultured with 2 mM phenobarbital (Sigma) for 1 day. Cells were washed twice with cold PBS followed by addition of 8 μM 7-ethoxyresorufin and μM dicumarol (Sigma) for 12 hours at 37℃. To 0.3 ml aliquots of culture medium, 0.2 ml ethanol was added, and samples were centrifuged for 10 minutes in a microcentrifuge to dissolve resorufin product, followed by fluorescence measurement at 530 nm (excitation) and 590 nm (emission). Purified resorufin (Sigma) was used to generate standard curves in the linear range, and data were normalized by measuring protein in aliquots with a Bio-Rad assay (Gupta et al., 1999).

Cytotoxicity assay

To demonstrate effects of conditioned medium from hESC-MECs on TNF-α cytotoxicity, 1.5×10^5 primary mouse hepatocytes isolated by collagenase perfusion of liver were plated in 24-well dishes in RPMI medium with 10% FBS and antibiotics. After overnight culture, cells were switched to conditioned medium plus 10 ng/ml TNF-α (Sigma) with or without 1–20 ng/ml VEGF (Sigma), followed by thiazolyl blue viability assays after 16–18 hours, as described previously (Joseph et al., 2005).

Induction of ALF in NOD/SCID mice

CB17.NOD/SCID^{prkdc} mice, 6–7 weeks old, were from Jackson Laboratories (Bar Harbor, ME). A total of 56 mice were studied in various groups for final experiments of hESC-MEC transplantation, including controls. Additional mice were studied for tumorigenicity assays (n=32). Mice were given three daily doses of i.p. Rif (75 mg/kg) and Phen (30 mg/kg) followed by one i.p. dose on day 4 of 125 or 160 mg/kg MCT. After 1 day, $4–6 \times 10^6$ cells were transplanted i.p. with 1 ml Cytodex 3 microcarriers (Amersham Biosciences, Piscataway, NJ). Sham-treated mice received vehicle and microcarriers. Encephalopathy was graded from 0 (absent) to 3 (coma) (Bandi et al. 2011). Animals were observed for up to 2 weeks. In some mice, 1 ml conditioned medium was injected i.p. daily for 3 days after Rif, Phen and 160 mg/kg MCT. In other mice, 1×10^6 hESC-MECs were injected into the portal vein. These mice were sacrificed 5 days after cell transplantation. Transplanted cells were identified by PCR for SRY and by in situ hybridization for alphoid satellite sequences in centromeres (Benten et al., 2006). For hepatic function determination in transplanted cells, glycogen and G-6-P were stained. To visualize GFP in LV-Alb-GFP transduced cells, tissues were fixed in PAF, equilibrated in 20% sucrose and frozen in methylbutane at −80℃, followed by immunostaining with rabbit anti-GFP (1:300, Molecular Probes) (Inada et al., 2008b). Sections were incubated with FITC-conjugated goat anti-rabbit IgG and counterstained with DAPI. For Ki67 and histone H2AX, tissues were fixed in 4% PAF followed by rabbit anti-Ki67 (1:750, Vector Laboratories, Burlingame, CA) or rabbit anti-phosphoS139 H2AX (1:300, ab2893; Abcam, Cambridge, MA), respectively, and secondary anti-Rabbit Alexa Fluor 546 (1:500, Molecular Probes), followed by counterstaining with DAPI.

Serum human albumin

Cell culture supernatant collected after 3 hours of plating and stored sera from recipients of transplanted cells were analyzed by human albumin immunoassay (Bethyl Laboratories, Montgomery, TX), according to the manufacturer's instructions.

Human cytokine arrays

Conditioned medium was analyzed by biotin label-based human antibody array I membrane for 507 human proteins (RayBiotech, Norcross, GA), according to the manufacturer's instructions.

Statistical analysis

Data were analyzed by Student's t-tests, log rank tests and ANOVA with Holm–Sidak post-hoc test. $P<0.05$ was considered significant.

Acknowledgements

Chaoying Zhang and Gertrude Ukpong provided technical assistance.

Funding

Supported in part by the National Institutes of Health [grant numbers R01 DK071111, P30 DK41296 and P30 CA13330] and funding from the New York State Stem Cell Science Program [grant number C024294]. S.B. was a Druckenmiller Fellow of the New York Stem Cell Foundation. Deposited in PMC for release after 12 months.

Supplementary material available online at
http://jcs.biologists.org/lookup/suppl/doi:10.1242/jcs.095372/-/DC1

References

Bandi, S., Joseph, B., Berishvili, E., Singhania, R., Wu, Y. M., Cheng, K. and Gupta, S. (2011). Perturbations in ataxia telangiectasia mutant signaling pathways after drug-induced acute liver failure and their reversal during rescue of animals by cell therapy. *Am. J. Pathol.* **178**, 161-174.

Baumgartner, D., LaPlante-O'Neill, P. M., Sutherland, D. E. and Najarian, J. S. (1983). Effects of intrasplenic injection of hepatocytes, hepatocyte fragments and hepatocyte culture supernatants on D-galactosamine-induced liver failure in rats. *Eur. Surg. Res.* **15**, 129-135.

Benten, D., Cheng, K. and Gupta, S. (2006). Identification of transplanted human cells in animal tissues. *Methods Mol. Biol.* **326**, 189-201.

Cho, J. J., Joseph, B., Sappal, B. S., Giri, R. K., Wang, R., Ludlow, J. W., Furth, M. E., Susick, R. and Gupta, S. (2004). Analysis of the functional integrity of cryopreserved human liver cells including xenografting in immunodeficient mice to address suitability for clinical applications. *Liver Int.* **24**, 361-370.

Dan, Y. Y., Riehle, K. J., Lazaro, C., Teoh, N., Haque, J., Campbell, J. S. and Fausto, N. (2006). Isolation of multipotent progenitor cells from human fetal liver capable of differentiating into liver and mesenchymal lineages. *Proc. Natl. Acad. Sci. USA* **103**, 9912-9917.

Demetriou, A. A., Whiting, J. F., Feldman, D., Levenson, S. M., Chowdhury, N. R., Moscioni, A. D., Kram, M. and Chowdhury, J. R. (1986). Replacement of liver function in rats by transplantation of microcarrier-attached hepatocytes. *Science* **233**, 1190-1192.

Ding, B. S., Nolan, D. J., Butler, J. M., James, D., Babazadeh, A. O., Rosenwaks, Z., Mittal, V., Kobayashi, H., Shido, K., Lyden, D., Sato, T. N., Rabbany, S. Y. and Rafii, S. (2010) Inductive angiocrine signals from sinusoidal endothelium are required for liver regeneration. *Nature* **468**, 310-315.

Fisher, R. A. and Strom, S. C. (2006). Human hepatocyte transplantation: worldwide results. *Transplantation* **82**, 441-449.

Grundmann, R., Koebe, H. G. and Waters, W. (1986). Transplantation of cryopreserved hepatocytes or liver cytosol injection in the treatment of acute liver failure in rats. *Res. Exp. Med. (Berl)* **186**, 141-149.

Gupta, S., Vemuru, R. P., Lee, C. D., Yerneni, P. R., Aragona, E. and Burk, R. D. (1994). Hepatocytes exhibit superior transgene expression after transplantation into liver and spleen compared with peritoneal cavity or dorsal fat pad: implications for hepatic gene therapy. *Hum. Gene Ther.* **5**, 959-967.

Gupta, S., Rajvanshi, P., Sokhi, R. P., Vaidya, S., Irani, A. N. and Gorla, G. R. (1999). Position-specific gene expression in the liver lobule is directed by the microenvironment and not by the previous cell differentiation state. *J. Biol. Chem.* **274**, 2157-2165.

Inada, M., Benten, D., Cheng, K., Joseph, B., Berishvili, E., Badve, S., Logdberg, L., Dabeva, M and Gupta, S. (2008a). Stage-specific regulation of adhesion molecule expression segregates epithelial stem/progenitor cells in fetal and adult human livers. *Hepatology Int.* **2**, 50-62.

Inada, M., Follenzi, A., Cheng, K., Surana, M., Joseph, B., Benten, D., Bandi, S., Qian, H. and Gupta, S. (2008b). Phenotype reversion in fetal human liver epithelial cells identifies the role of an intermediate meso-endodermal stage before hepatic maturation. *J. Cell Sci.* **121**, 1002-1013.

Joseph, B., Bhargava, K. K., Tronco, G. G., Kumaran, V., Palestro, C. J. and Gupta, S. (2005). Regulation of hepatobiliary transport activity and noninvasive identification of cytokine-dependent liver inflammation. *J. Nucl. Med.* **46**, 146-152.

Makowka, L., Falk, R. E., Rotstein, L. E., Falk, J. A., Nossal, N., Langer, B., Blendis, L. M. and Phillips, M. J. (1980). Cellular transplantation in the treatment of experimental hepatic failure. *Science* **210**, 901-903.

Massie, I., Selden, C., Hodgson, H. and Fuller, B. (2011) Cryopreservation of encapsulated liver spheroids for a bioartificial liver: reducing latent cryoinjury using an ice nucleating agent. *Tissue. Eng. Part C Methods* **17**, 765-774.

Nakagawa, M., Koyanagi, M., Tanabe, K., Takahashi, K., Ichisaka, T., Aoi, T., Okita, K., Mochiduki, Y., Takizawa, N. and Yamanaka, S. (2008). Generation of induced pluripotent stem cells without Myc from mouse and human fibroblasts. *Nat. Biotechnol.* **26**, 101-106.

Olivier, E. N., Rybicki, A. C. and Bouhassira, E. E. (2006). Differentiation of human embryonic stem cells into bipotent mesenchymal stem cells. *Stem Cells* **24**, 1914-1922.

Phillips, B. W., Hentze, H., Rust, W. L., Chen, Q. P., Chipperfield, H., Tan, E. K., Abraham, S., Sadasivam, A., Soong, P. L., Wang, S. T. et al. (2007). Directed differentiation of human embryonic stem cells into the pancreatic endocrine lineage. *Stem Cells Dev.* **16**, 561-578.

Quaglia, A., Portmann, B. C., Knisely, A. S., Srinivasan, P., Muiesan, P., Wendon, J., Heneghan, M. A., O'Grady, J. G., Samyn, M., Hadzic, D. et al. (2008). Auxiliary transplantation for acute liver failure: Histopathological study of native liver regeneration. *Liver Transpl.* **14**, 1437-1448.

Ria, R., Piccoli, C., Cirulli, T., Falzetti, F., Mangialardi, G., Guidolin, D., Tabilio, A., Di Renzo, N., Guarini, A., Ribatti, D. et al. (2008). Endothelial differentiation of hematopoietic stem and progenitor cells from patients with multiple myeloma. *Clin. Cancer Res.* **14**, 1678-1685.

Rodaway, A. and Patient, R. (2001). Mesendoderm. An ancient germ layer? *Cell* **105**, 169-172.

Thomson, J. A., Itskovitz-Eldor, J., Shapiro, S. S., Waknitz, M. A., Swiergiel, J. J., Marshall, V. S. and Jones, J. M. (1998). Embryonic stem cell lines derived from human blastocysts. *Science* **282**, 1145-1147.

Wang, L. J., Chen, Y. M., George, D., Smets, F., Sokal, E. M., Bremer, E. G. and Soriano, H. E. (2002). Engraftment assessment in human and mouse liver tissue after sex-mismatched liver cell transplantation by real-time quantitative PCR for Y chromosome sequences. *Liver Transpl.* **8**, 822-828.

Wu, S. M. and Hochedlinger, K. (2011). Harnessing the potential of induced pluripotent stem cells for regenerative medicine. *Nat. Cell Biol.* **13**, 497-505.

Zaret, K. S. (2008). Genetic programming of liver and pancreas progenitors: lessons for stem-cell differentiation. *Nat. Rev. Genet.* **9**, 329-340.